The 8th European Congress on Computational Methods in Applied Sciences and Engineering
ECCOMAS Congress 2022
5 – 9 June 2022, Oslo, Norway

A VALIDATION PROGRAM FOR DYNAMIC HIGH-LIFT SYSTEM AERODYNAMICS

JOCHEN WILD[1], HENNING STRÜBER[2], FRÉDÉRIC MOENS[3], BART VAN ROOIJEN[4] & HANS MASELAND[5]

[1] German Aerospace Center (DLR)
Lilienthalplatz 7,38108 Braunschweig, Germany
email: jochen.wild@dlr.de

[2] Airbus Operations GmbH
Bremen, Germany,
email: henning.strueber@airbus.com

[3] French Aerospace Lab (ONERA)
Meudon, France
email:frederic.moens@onera.fr

[4] German-Dutch Wind Tunnels (DNW)
Marknese, The Netherlands
email: bart.van.rooijen@dnw.aero

[5] Royal Netherlands Aerospace Centre (NLR)
Amsterdam, The Netherlands
email: hans.maseland@nlr.nl

Key words: Aerodynamics, Unsteady, High-Lift Systems, CFD, Wind Tunnel, Validation.

Summary *The feasibility of laminar flow control technology for future wing is bound to the development of a leading edge high-lift system that complies with the requirements on smooth surfaces to enable maintaining the laminar boundary layer flow, such as a Krueger flap. Although in principle the aerodynamic performance of a Krueger flap is known, the unsteady behaviour of the flow during deployment and retraction is completely unknown. This is as even more important as during deployment the Krueger flap is exposed to highly unfavourable positions perpendicular to the flow. To mitigate the risk of unfavourable aircraft behaviour, it is therefore expected that a Krueger flap has to be deflected significantly fast and may trigger unsteady aerodynamic effects.*
The European H2020 project UHURA, running from September 2018 to August 2022, has been focusing on the unsteady flow behaviour around such high-lift system and will first time deliver a deeper understanding of critical flow features at this type of high-lift device during their deployment and retraction together with a validated numerical procedure for its simulation. UHURA performed detailed experimental measurements in several wind tunnels to obtain a unique data set for validation purposes of Computational Fluid Dynamics (CFD) software, including detailed flow measurements by Particle Image Velocimetry (PIV) and other optical measurement technologies. Advanced CFD methods promising significant improvements in the

design lead time have been applied and validated against this database to obtain efficient and reliable prediction methods for design.
This first contribution within the Special Technology Session provides an overview on the project. While the simulation activities are detailed in the forthcoming presentations, this presentation focusses on the experiments conducted to obtain a unique database for the validation of simulation methods for this kind of unsteady flows. Finally, an outlook is given on the validation and exploitation methodology applied in the last period of the project.

1. INTRODUCTION

Laminar wing technology is expected to be the most significant aerodynamic contribution to aircraft drag reduction and fuel savings of next generation transport aircraft. Nevertheless, this assumption is based on some premises: i) it is assumed that the low speed performance in high-lift configuration is retained avoiding an increase in wing area to achieve the required approach speed; ii) the high-lift system at the leading edge doesn't disturb the surface quality needed for laminar flow at least at the upper side preventing classical slat devices to be installed; and iii) the wing surface stays clean from further disturbances introduced by insects, dust or dirt during ground an low altitude operations preventing laminar flow to develop.

For such aircrafts Krueger flaps are currently the most favoured high-lift system concept at the leading edge of a transport aircraft wing. The Krueger flap originates back to the 1940's when Werner Krueger reported on a new high-lift device called the "nose split flap" [1]. The first Boeing jet airliners B707, B727, B737-100 and B747 all used Krueger flaps as their leading edge device [2] (see Figure 1).

Figure 1: Krueger flaps inboard of a Boeing B707 (left – image obtained from www.wikiwand.com) and the outboard variable camber Krueger flap of the Boeing B747 (right – image obtained from www.wired.com © Jason Paur)

Especially the vented Krueger flap with or without folding bull-nose is most likely the high-lift system enabling laminar wing technology. Aside the high-lift performance, it serves as a device for shielding the wing against contamination by insects or other pollutants during low altitude flight. Previous studies already showed the feasibility in terms of aerodynamics and wing integration [3].

A Krueger flap deploys from the lower side of the wing and moves around the leading-edge until it reaches a position in front and slightly above the wing leading edge. Figure 2 depicts

the Krueger flap developed in the DeSiReH project [4] at several positions during this deployment. Especially the positions when the Krueger flap is perpendicular to the flow bears possible risks during operation. When the Krueger flap is passing the leading-edge it may shield the wing from the flow, thus causing a sever loss in lift. It is therefore required not to move all Krueger flaps along the span at the same time. Even older aircraft having sealed Krueger flaps operated in sequential mode – e.g. the Boeing B707 seen in Figure 3 – or in groups like the Boeing B747.

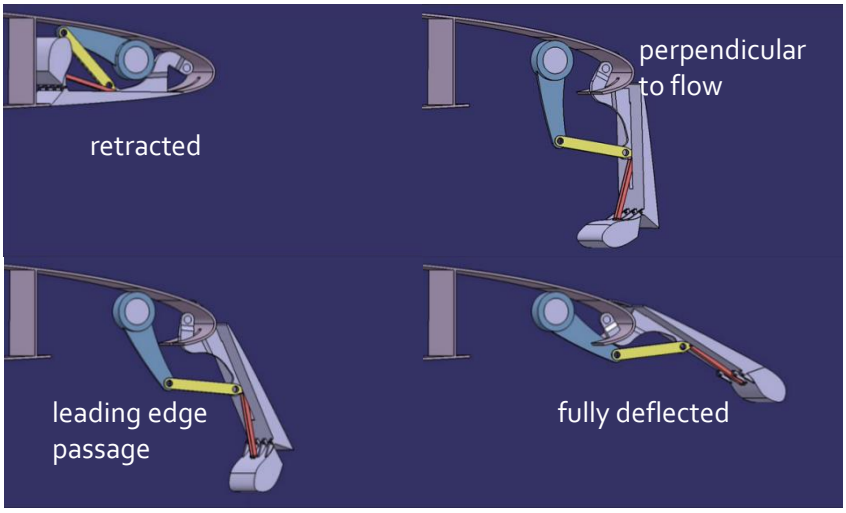

Figure 2: Vented folding bull-nose Krueger flap at specific positions on the deployment path

Figure 3: (left) sealed Kruger flap at the Boeing B707 operated sequentially (image obtained from airliners.net © Teemu Tuuri); (right) inboard Krueger flap at the Boeing B747 operated in groups (image obtained from youtube.com © user/Jet3TV)

In any case, the passage around the leading case poses an additional criticality. For this reason, additional challenges arise, which should be addressed during the design. The limited overall deployment time requires an increase of the deployment speed. The lower number of flaps is operated at the same time the higher is the required angular speed to deflect the full system in an acceptable time within about 20 to 30 seconds. At such high rotational speeds, unsteady effects on the flow start to get likely. In order to take these effects into account during design, it is necessary to validate the simulation methods in this flow regime. Since the movement of the 3 Krueger flap significantly differs by the amount of movement and the

characteristic speed from other unsteady flow problems, a new validation approach is needed to get confidence into the simulation methods.

2. PROJECT SCOPE AND TESTING STRATEGY

The UHURA project (UHURA = Unsteady High-Lift – Unsteady RANS Validation) is a Research Innovation Activity (RIA) funded within the Horizon 2020 Programme of the European Commission. It aims at validation of unsteady flow simulation methods for the designated type of unsteady flow problem. After an initial phase of designing the appropriate flow problem, the project in parallel matures methods for calculating the flow by different means of Computational Fluid Dynamics (CFD) and sets up a series of wind tunnel tests to obtain high-quality validation data.

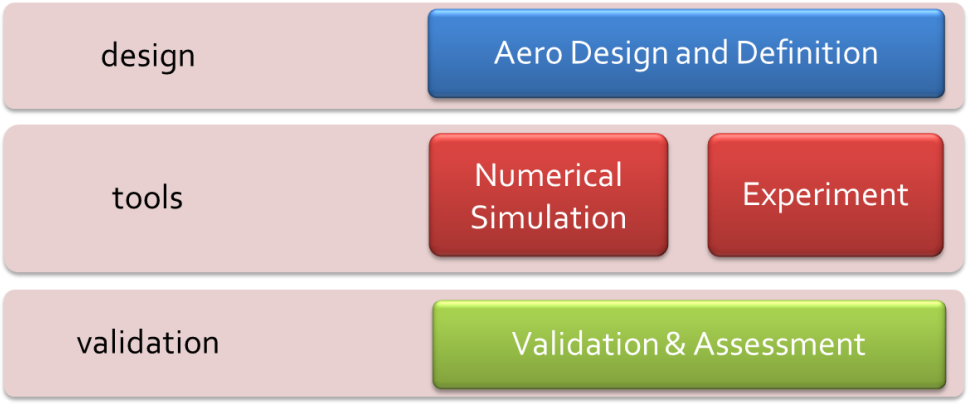

Figure 4: Project structure of the UHURA project

The project has been structured in three phases (Figure 4). The first phase concentrated on the specification of the investigated specimen. This included the aerodynamic design of a Krueger flap for the designated laminar wing airfoil (see presentation in this session [5]), the definition of the kinematics for moving the Krueger flap from retracted to deflected position as well as establishing further requirements on the dynamics of the deflecting motion, especially the required deflection times. In the second phase, the numerical simulation methods were matured for the simulation of the deflecting Krueger device. This aimed to gain of some best practice in terms of mesh generation and solver settings. In parallel the wind tunnel experiments were setup and performed, including modifying the wind tunnel models by incorporating a controlled moveable Krueger device into the leading edge of existing high-lift airfoil models, and maturing and synchronizing the time-resolved measurement techniques applied. The final phase is dedicated to numerically simulate the preformed experimental conditions including the measured deployment schedules of the Krueger flap motion and to compare with the detailed experimental database obtained in the wind tunnel experiments for validating the numerical tools.

Wind tunnel tests are foreseen in three different wind tunnels with two models to cover a broad range of conditions including variation of Krueger span (full span – part span), wing sweep angle and Reynolds number. The used airfoil geometry is derived from the DLR-F15 high-lift geometry [6] equipped with a modified leading edge of a laminar wing airfoil denoted by the extension -LLE [7] (Figure 5). This leading edge together with the Krueger flap designed

in the project was adopted to two specific wind tunnel models. The baseline DLR-F15 wind tunnel model is a 600m chord high-lift model with a span of 2.4-2.8 m. This model was used in the ONERA L1 wind tunnel in a 2D wall-to-wall setup (Figure 6 left) and the DNW-NWB wind tunnel as a cantilever wing with wing sweeps of 0 deg and 23 deg (Figure 6 middle). The larger variant for swept installation DLR-F15*LS* is a 2:1 upscale with 1.2 m chord and 7 m span and was mounted at a sweep angle of 30 deg in the DNW-LLF wind tunnel (Figure 6 right). With this wind tunnel strategy, the project was able to create a consistent database on the aerodynamics of a moving Krueger device including the effects of Reynolds number and wing sweep.

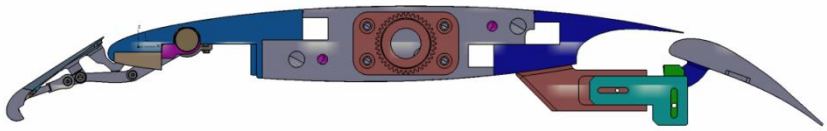

Figure 5: sectional view of the DLR-F15 wind tunnel model equipped with laminar leading Edge (-LLE) and movable Krueger flap device on realistic kinematics

Figure 6: wind tunnel model installations used in the UHURA Project: (left) DLR-F15-LLE mounted wall-to-wall in ONERA L1; (middle) DLR-F15-LLE mounted as swept cantilever wing in DNW-NWB; (right) DLR-F15LS-LLE mounted as swept wing in the open test section of DNW-LLF

3. VALIDATION DATABASE FOR DYNAMIC KRUEGER FLAP MOTION

A major objective of the UHURA project is the creation of a database with aerodynamic flow data for the unsteady flow properties of a fast-moving Krueger flap high-lift device. by combining the different models and tunnels, further influence factors shall be evaluated that cannot be easily done with a single entry. By using two models with same shape at different scale, the Reynolds number effect can be differentiated from the effect of wind speed and Mach number. By comparing full-span and part span Krueger flaps, effects of the limited span during motion and its effect on the dynamic behaviour is accessible. Further, the effect of wing sweep is evaluated by the different setups.

In order to be comparable in all these data sets, it is important to establish a common basis and a common reference. This has been done by prescribing the pressure distribution of a 2D CFD simulation at an angle of attack of 6 deg as the designated operating point. During wind tunnel tests, first this condition has been established by tuning the angle of attack so that the corresponding target pressure distribution with retracted Krueger flap is obtained. The retracted Krueger flap pressure distribution has been used her to avoid uncertainties due to Krueger deformation und wind load, which are part of the data analysis.

Another aspect for being comparable between the different tunnel entries is the correlation of the dynamic behaviour in terms of time scales. Starting with the nominal wind speeds of 30 and 45 m/s for the two-dimension flow, the wind speeds at the swept wing experiments were increased to obtain the same convective time over the wing, which is achieved by retaining the wing normal wind velocity. Doing so, no impact is expected due to Mach number variation and the time scales for the dynamic motion of the Krueger can be kept as is. For the DNW-LLF experiments with the 2:1 upscaled model, the motion time scales are half of those of ONERA L1 and DNW-NWB experiments in order to achieve the same dimensionless time relations.

3.1. Tests at ONERA L1 wind tunnel

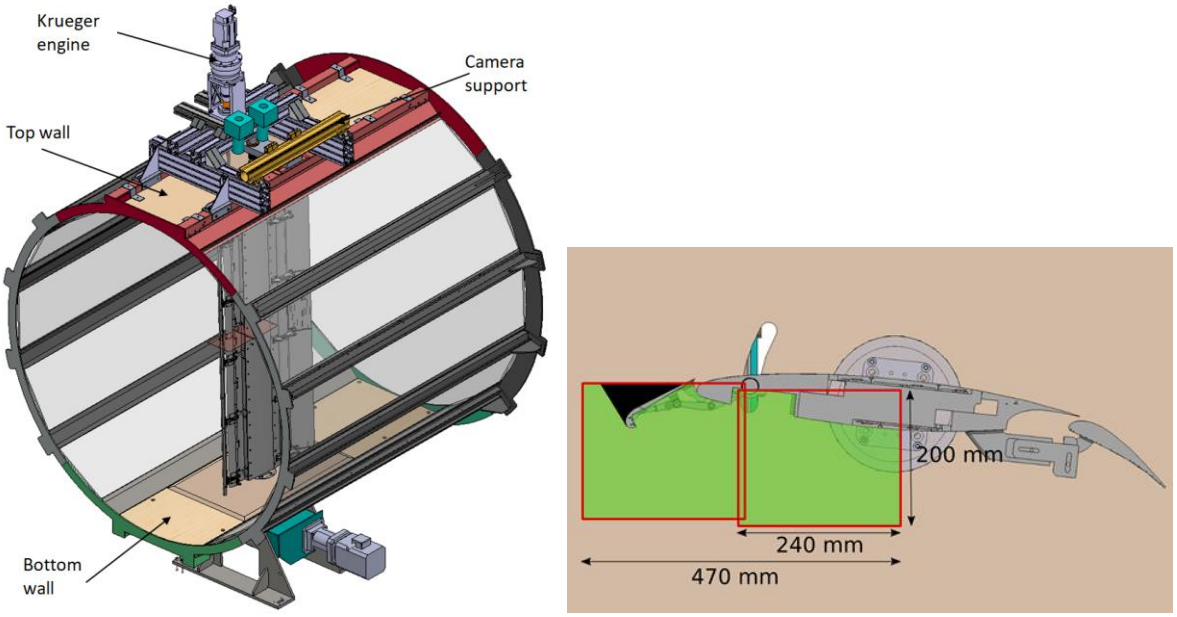

Figure 7: (left) general arrangement of wind tunnel setup of DLR-F15-LLE in ONERA-L1; (right) PIV image position relative to model cross section

The emphasis of the ONERA L1 test is on the one side to achieve the most two-dimensional data by using a full span installation of the Kreuger flap spanning the whole model from wall to wall. Since the optical access to the closed test section is given, high-quality flow measurement by Particle Image Velocimetry (PIV) is a second major aim of the test campaign. The test campaign was executed in two entries. The first entry in October 2020 served as a check-out test for the measurement techniques and the synchronization strategy. It also served as a check-out of the model. In fact, the first campaign unveiled some mechanical jitter in the

mechanics that was improved for the second entry in September/October 2021. In this second phase the productive measurements and the majority of the PIV data has been conducted.

In this test setup, the DLR-F15-LLE model wing was mounted vertically in the dodecagonal test section of the ONERA L1 wind tunnel at ONERA in Lille, France (Figure 7 left). The wing incidence was controlled by a motor below the bottom wall, while on the top, the drive unit for the Krueger flap was installed. Just aside the Krueger drive unit, the two CMOS cameras for the 2D2C PIV setup were installed. The cameras recorded two adjacent windows on the pressure side of the wing capturing the motion path of the Krueger flap up to half the wing chord (Figure 7 left).

Beside the PIV installation, the applied measurement techniques included static pressure measurements by 139 static pressure taps connected to multi-channel pressure scanners, dynamic pressure measurements by 26 Bosch BMP388 MEMS sensors and five Kulites for reference. From the drive system the angular position of the drive shaft was transiently recorded.

Table 1: test conditions of the wind tunnel test in ONERA L1

general		
wind speed	[m/s]	30; 45
static cases		
angle of attack	[deg]	0 … $\alpha(C_{L,max})$ + 5 deg
Krueger flap angle	[deg]	0; 37.5; 75; 112.5; 142.9
dynamic cases		
angle of attack	[deg]	6
deflection time	[s]	1; 2; 4
hold time	[s]	1; 2

Table 1 lists the test conditions where data has been obtained. First, for the two given wind speeds static data points have been acquired by an angle of attack sweep from zero incidence up to 5 degrees beyond maximum lift coefficient. From this the reference angle of attack of 6 degrees was established by comparison to the target pressure distribution for all further measurements with deployed Krueger flap. Second, at this incidence, statically deployed Krueger positions at 5 steps from fully retracted to fully deflected have been measured. For the turbulent statistics up to 2500 snapshots have been sampled. Figure 8 exemplarily shows the time averaged relative axial velocity and the turbulent in-plane kinetic energy content.

The major time of the test was spent with the recording of unsteady transient flow data by pressure and PIV. PIV image acquisition was possible at a rate of 5 Hz. In order to get a sufficient angular resolution of the motion, the PIV image acquisition at high deployment speeds were repeated with a phase shift so that at least 20 snapshots per deployment cycle were obtained. This results in an angular resolution of about 7 degrees Krueger deployment. Each phase angle of a motion cycle was recorded at least by 300 snapshots for a statistical evaluation of phase averaged data. Thus, for the shortest deflection time of 1 second, in total 1200 deployment and retraction cycles have been sampled. For the longest deflection time of 4 seconds the acquisition frequency was high enough to avoid the phase shift and repetition. Although this reduces the number of cycles, the overall measurement time is nevertheless the same.

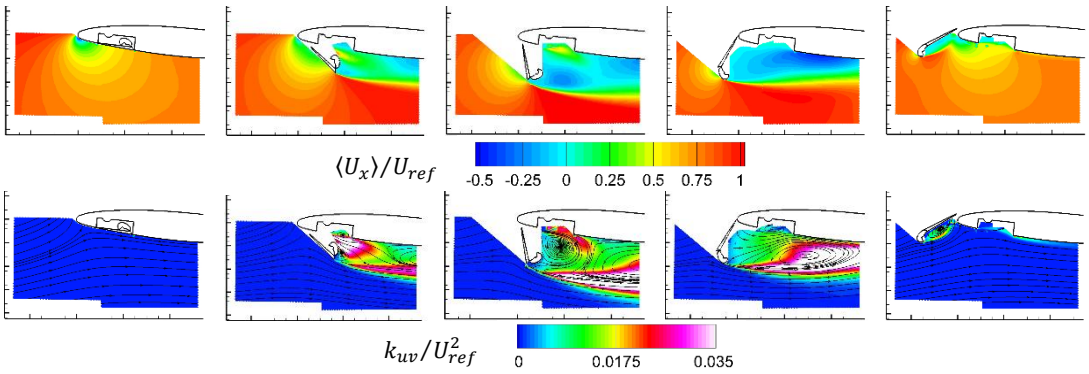

Figure 8: PIV results at static Krueger flap positions left to right: 0°, 37.5°, 75°, 112.5°, 142.9°; V_∞ = 45 m/s. (Upper row) rel. axial velocity component; (lower row) turbulent kinetic in-plane energy

A sufficiently high accuracy of data acquisition for this high number of runs was only possible with a sophisticated synchronization of all measuring systems, namely the Krueger drive controller, the PIV system, the MEMS system and the transient recording. This has been achieved by TTL handshake signals thus that the PIV acquisition and the motion initiation were synchronized at each deflection cycle. The ONERA L1 test here also served as a check-out of the architecture if the overall measurement and test system setup and was used in the same or similar way in the other facilities DNW-NWB and DNW-LLF.

3.2. Tests at DNW-NWB wind tunnel

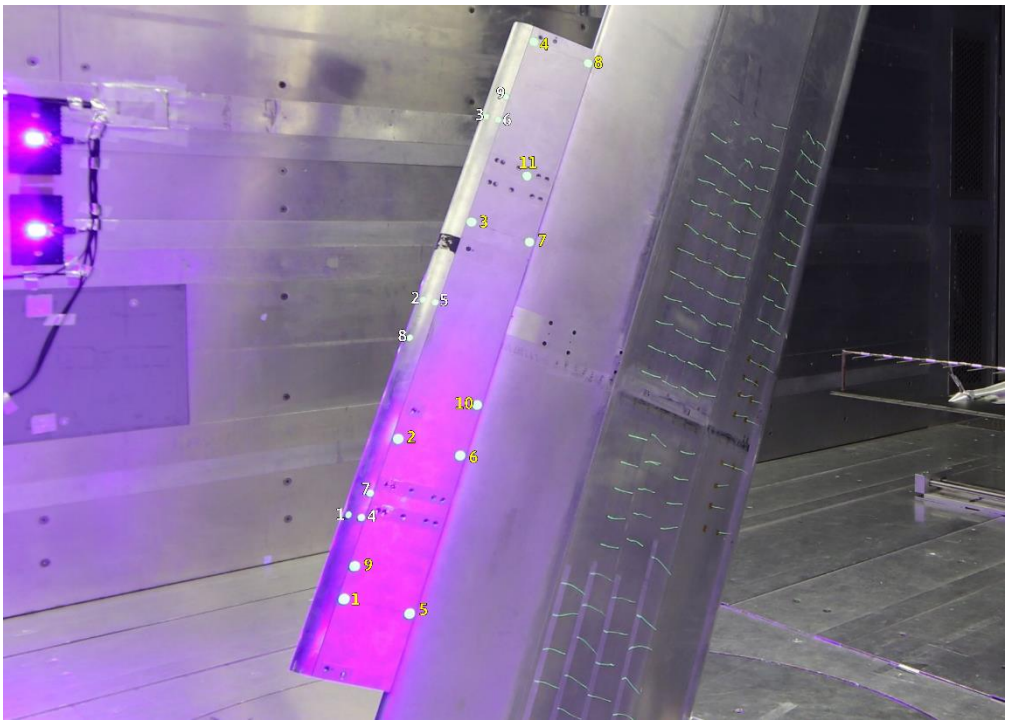

Figure 9: DLR-F15-LLE model with deflected Krueger flap with marker arrangement for optical position and deformation measurement of the Krueger flap by SPR mounted as cantilever wing with 23 degree wing sweep in the closed test section of DNW-NWB

The test at DNW-NWB concentrated on obtaining pressure and transient data for the variation of the dynamic motion characteristics and to analyse the effect of wing sweep on a single deflected part-span Krueger element. This test was conducted in March/April 2021.

Due to the model installation, the only the centre part of the Kreuger spanning 800 mm of span was actuated. No PIV was acquired in this test, but the deformation of the Krueger was recorded by use of a Stereo Pattern Recognition (SPR) system (see Figure 9) that is targeted for the DNW-LLF entry, too. In addition, the static conditions were additionally measured in the wake of the airfoil model by a traversable wake rake. The wing was installed at two different sweep angles, 0 degree and 23 degree, the latter being the mechanical limit of the model support.

Table 2 lists the test conditions examined in the DNW-NWB test. It is emphasized again that in order to retain the dynamic characteristics, the wing leading edge normal velocity has been kept constant for tests with and without wing sweep. Thus, the wind speed with the swept wing was increased by a factor of $1/\cos(\varphi)$ compared tot the straight wing. The reference angle of attack for all dynamic and static Krueger deflections were set to 8 degrees based on a comparison of the pressure distribution measured in ONERA L1 and DNW NWB. This is somehow the angle of attack correction for the cantilever wing installation. Incidentally, this angle correction was the same of 0 deg and 23 deg sweep, which has been established separately.

Table 2: test conditions of the wind tunnel test in DNW-NWB

general		
wing sweep φ	[deg]	0; 23
wing normal wind speed $V_N = V_\infty \times \cos(\varphi)$	[m/s]	30; 45
static cases		
angle of attack	[deg]	–5 deg … $\alpha(C_{L,max})$ + 5 deg
Krueger flap angle	[deg]	0; 37.5; 75; 112.5; 142.9
dynamic cases		
angle of attack	[deg]	8
deflection time	[s]	1; 2; 4;
hold time	[s]	1; 2; 4
drive acceleration	[deg / s²]	165; 300; 500; 1000

Figure 10 exemplarily shows the time histories of the MEMS pressure sensors of Krueger flap and main wing recorded during one specific deployment and retraction cycle. On the left image showing the pressure channels on the Krueger one sensor is highlighted by a thicker line, showing the non-symmetric nature of the signal indicating hysteresis and dynamic effects even for the shown slow motion at the longest deflection time of 4 seconds.

This instantaneous data is phase averaged over 5 to 8 repetitions and then synchronized with the tunnel and drive data to obtain the dynamic pressure distributions with actual deflected positions as shown in Figure 11. Clearly seen is the overshoot of the suction pressure in the second snapshot where the suction on the wing supersedes even the steady condition. This is attributed to the dynamic acceleration of the flow due to the Krueger pushing the flow around the leading edge.

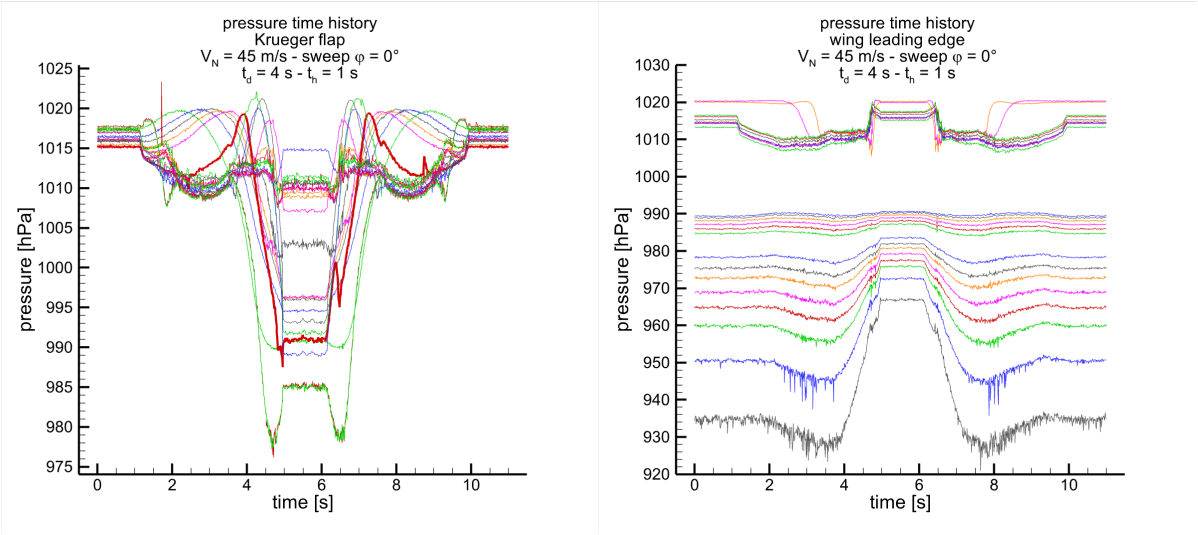

Figure 10: time histories of dynamic pressure measurements using MEMS for a specifie deployment schedule: (left) Krueger flap; (right) main wing leading edge

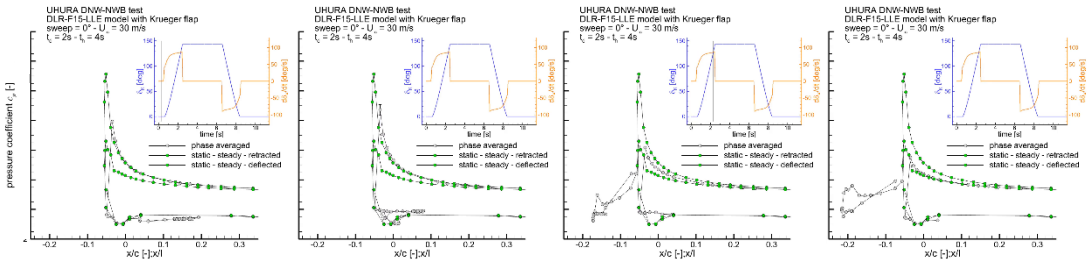

Figure 11: snapshots of the analysed pase-averaged pressure distributions from MEMS data synchronized with tunnel data and position measurements

3.3. Tests at DNW-LLF wind tunnel

For the third test campaign, the larger DLR-F15LS-LLE model was mounted in the open 6x8 m² test section in the Large Low-speed Facility DNW-LLF in Marknese, The Netherlands. The campaign was conducted in two entries. In April 2021 the data acquisition mainly concentrated on pressure, position and deformation measurements using SPR and discrete accelerometers on the Krueger flap were performed, while the second entry in April 2022 concentrated on acquiring flow field information by PIV.

The larger model DLR-F15LS-LLE is a 2:1 upscale of the model used in ONERA L1 and DNW-NWB. Thus, at the same flow condition the double Reynolds number is obtained. The Kreuger flap in this model spans 3 m and is like for the cantilever wing in DNW-NWB a part-span arrangement. Due to the larger size, the Krueger is now driven by two synchronized motors from both sides. Figure 12 shows on the left side the installed model with the SPR markers in the first entry and on the right side the PIV arrangement with the laser light sheet illuminating the wing in a centre section.

Due to its size the DLR-F15LS-LL model allowed for a denser instrumentation for pressure measurements. While the MEMS arrangement has been retained from the small model, the number of pressure tabs in the centre section has twice the number of pressure ports increasing

the overall accuracy of the pressure distribution. In addition, two more pressure sections are installed each 1m to the left and right providing some information on the spanwise variation of the flow along the Krueger span. Further, in this model setup the pressure scanners were implemented into the wing leading edge providing only short pressure tubing. By this, the low frequency dynamics of the pressure in were measured at a 100 Hz simultaneously to the MEMS sensors in partly overlapping areas by a second system thus providing additional reliability in the MEMS technique.

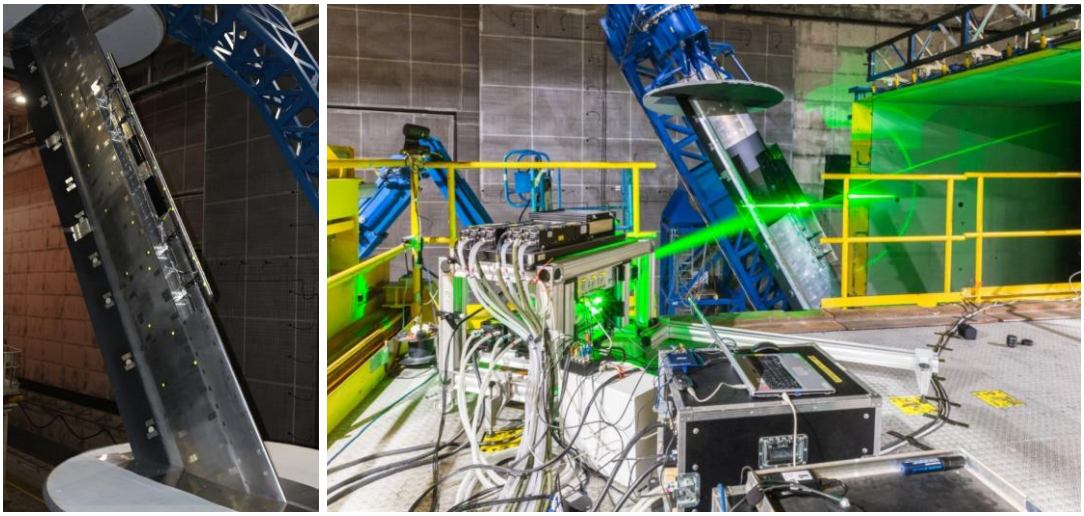

Figure 12: installation of model and optical measurement techniques in the DNW-LLF facility: (left) SPR markers on the wing with deployed part-span Krueger flap; (right) laser system illuminating the PIV section in the centre of the part-span Kreuger flap

Table 3: test conditions of the wind tunnel test in DNW-LLF

general		
wing sweep φ	[deg]	30
wing normal wind speed $V_N = V \times \cos(\varphi)$	[m/s]	30; 45
static cases		
angle of attack	[deg]	-2 … 17
Krueger flap angle	[deg]	0; 37.5; 75; 112.5; 142.9
dynamic cases		
angle of attack	[deg]	15.7
deflection time	[s]	2; 4; 8
hold time	[s]	1

The test conditions in DNW-LLF are listed in Table 3. Like for the previous campaigns, the wind speed was selected to achieve a similar wing leading edge normal velocity. The deflection times are doubled in comparison to the previous campaigns accounting for the 2:1 upscale to achieve similar dimensionless time scales. The pressure distribution again has been adjusted to best match the target pressure distribution. Due to the wing sweep, the rotation axis along the wing span instead of perpendicular to the flow, and due to the open test section, in the DNW-LLF the angle of attack was adjusted to 15.7 degrees.

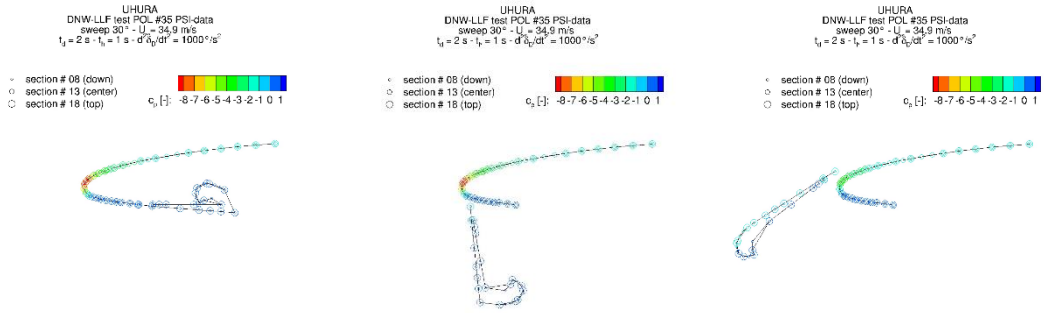

Figure 13: snapshots of the analysed pase-averaged pressure distributions from PSI data synchronized with tunnel data and position measurements

As an example, Figure 13 shows the derived geometric pressure tap positions coloured by the actual pressure coefficient for the three pressure wing sections on the wing and the two on the Krueger marked by the size of the circle. Beside the variation of the pressure between retracted and deflected also the spanwise variation is seen to be minimal, which is a result of the relatively high aspect ratio of the 3 m Krueger panel span.

In the second campaign four cameras were used to obtain 2D3C stereo PIV images at two acquisition windows similar to the ones in ONERA L1 at a sampling rate of 20Hz using four laser sources. Due to the higher sampling frequency and the lowered deflection rates, no phase shifted repetition was required. In total 1000 samples have been obtained for each phase-locked position for the shortest deployment time of 2 seconds and 500 samples for the rest. 600 GB of raw PIV data have been recorded and are still in the processing

4. SIMULATION AND VALIDATION STRATEGY

The final project phase currently under progress is now dealing with the validation of the numerical methods using the described wind tunnel data. Several partners analyse their simulations with different methods of CFD. **Table 4** lists the various partners of the project, their applied CFD methodology and the respective focus of related wind tunnel test entry. The methods range from application of state-of-the-art unsteady Reynolds-averaged Navier-Stokes solver (uRANS) based on the Chimera – or overset – approach, scale-resolving methods of blended RANS and Large Eddy Simulation (LES) methods, Immersed Boundary Methods (IBM), and Lattice Boltzmann Methods (LBM). Some partners additionally couple with Computational Structure Mechanics (CSM) methods by Fluid-Structure Interaction (FSI) coupling to account for the model deformation.

It is not aim of this contribution to go into details here. This is done by the other following contributions to this Special Technology Session. The first summarizes the lessons learned applying the Chimer method [8], the second values the benefit of time resolving methods [9], and the last the experience with applying a completely different simulation approach with Lattice Boltzmann methods.

Just as a teaser here for the upcoming comparison of experimental and numerical simulation data, Figure 14 presents the PIV images obtained from static measurements with retracted and deployed Krueger flap within the first ONERA L1 wind tunnel test overlaid on the flow fields obtained by the corresponding CFD simulations. This first and rough comparison raises high

expectations both on the quality of experimental data and on the maturity of simulation methods to handle the designated flow.

Table 4: work share distribution between project partners for validation of the different methodologies using different wind tunnel entry data

	ONERA L1	DNW-NWB	DNW-LLF	OBJECTIVE/FOCUS ON	SIMULATION APPROACH	MESHING APPROACH
CIRA	√		√	Assessment of different approaches (Multiblock Dynamic mesh vs. Immersed Boundaries). Assessment of IB method (Static FSI, Dynamic and Dynamic FSI) for Krueger loads estimation.	URANS, Static, Dynamic and coupled FSI aero-elastic simulations.	Multiblock structured dynamic mesh and non-conformal mesh coupling. Immersed Boundaries method with (dynamic) local grid refinement.
DLR		√	√	Scaling effect on swept wing configurations. Relation between displacement and flow velocities.	URANS, Static and Dynamic aerodynamic simulations	Unstructured + Chimera / sliding interfaces
DASSAV			√	Assessment of critical loads estimation during the deployment phase.	Static-Unsteady - 2.5D Delayed Detached Eddy Simulation	In-house Aether code for unstructured multi-block meshes
IBK	√		√	Assessment of Static FSI and dynamic FSI coupling and modeling.	CSM coupling to CIRA's Immersed Boundaries flow solver	CSM for IB method (CIRA)
INTA	√			Assessment of the LBM methodology. Characterization of the flow physics during the deployment/retraction phases.	Static-Unsteady and Dynamic LBM with Wall modelled LES (XFlow)	Cartesian mesh based on dynamic Octree and box refinement on selected areas.
KTH	√		√	Detailed turbulent flow field and dynamics including FSI at particular critical deployment stages.	Dynamic-Unsteady URANS. Static-Unsteady hybrid RANS-LES including FSI.	Unstructured grid deformation and local remeshing.
NLR	√	√	√	Temporal aspects of the flow dynamics (interactions of viscous flow regions and unsteady, separated flow). Characterization of the aero-loads.	URANS, Static & Dynamic FSI aero-elastic simulation (one or two-way fluid-structure coupling)	Multiblock structured, deformation of non-overlapping conformal blocks and discontinuous (sliding) grid interfaces. Local grid refinement/adaptation & local splitting of blocks .
ONERA	√	√		Flow simulations of device deployment and loads estimate by using ONERA's in-house solver elsA.	Static-Unsteady and Dynamic-Unsteady RANS, dynamic mesh motion for rigid body	Chimera grid with dynamic mesh motion.
VZLU	√		√	Improve the knowledge of the dynamics of the turbulent flow. Effect of Krueger flap deformation, evaluation of deflection rate effects.	Static&Dynamic-Unsteady/Dynamic FSI, URANS. Improvement of local flow field knowledge by hybrid RANS-LES.	Mesh deformation together with local re-meshing

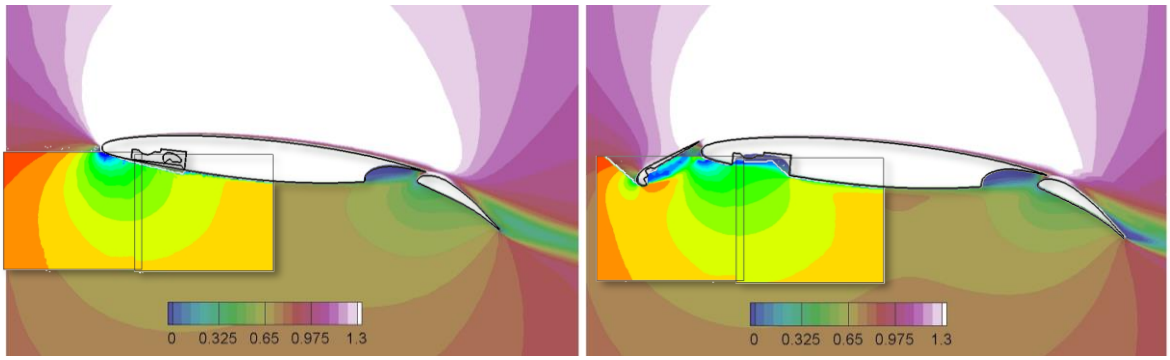

Figure 14: Overlay of time averaged PIV image of static Krueger position with Flow field obtained from CFD simulation: (left) retracted Krueger flap; (right) fully deflected Kreuger flap

5. CONCLUSION

The project UHURA aimed at validating numerical simulation methods for the aerodynamics of moving high-lift devices. These validate methods shall further on help mitigating critical flow states at innovative high-lift systems, especially Krueger flaps to be implemented at laminar technology wings.

The project created a unique and comprehensive database for such flows by conducting 5 wind tunnel campaigns in three different tunnels using two different models of same shape but different scale. It cannot be emphasized enough that this was a very special journey since the COVID-19 pandemic mostly prevented travelling and thus all the tests performed in a cooperative way had to be conducted with remote support only.

In total, 34 GigaByte of time resolved data have been collected, not yet including the PIV and SPR images. This database is now ready for supporting validation activities of numerical simulation methods. This validation has started and first results are presented in the following contributions to this Special Technology Session on "Unsteady Simulation of High-Lift System Aerodynamics".

ACKNOWLEDGMENT

The project leading to this publication has received funding from the European Union's Horizon 2020 Research and Innovation Framework Programme under the research and innovation programme under grant agreement No 769088.

Further on, special thanks are attributed to all the contributing staff not explicitly named here, mainly all the colleagues contributing to the project – whether in simulations or experiment, all the colleagues at the testing facilities and all the colleagues running the highly innovative measurement technologies.

REFERENCES

[1] Krüger, W. Über eine neue Möglichkeit der Steigerung des Höchstauftriebes von Hochgeschwindigkeitsprofilen, AVA-Bericht 43/W/64, (1943).

[2] Rudolph, P.K.C. High-Lift Systems on Commercial Subsonic Airliners, NASA-CR-4746 (1996).

[3] Boeing Commercial Airplane Group, High Reynolds Number Hybrid Laminar Flow Control (HLFC) Flight Experiment - II. Aerodynamic Design, NASA CR-1999-209324 (1999).

[4] Strüber, H. and Wild, J. Aerodynamic Design of a High-Lift System Compatible with a Natural Laminar Flow Wing within the DeSiReH Project, *29th Congress of the International Council of the Aeronautical Sciences* (2014) Paper-ID ICAS 2014-0300.

[5] Iuliano, E., Quagliarella, D. and Wild, J. Krueger High-Lift System Design Optimization, *The 8th European Congress on Computational Methods in Applied Sciences and Engineering - ECCOMAS Congress 2022* (2022), Paper-ID 2241.

[6] Wild, J. Mach and Reynolds Number Dependencies of the Stall Behavior of High-Lift Wing Sections. *Journal of Aircraft* (2013) **50**(4):1202-1216. doi:10.2514/1.C032138

[7] Ciobaca, V. and Dandois, J. High Reynolds Number High-Lift Airfoil Testing with Flow Control. *35th AIAA Applied Aerodynamics Conference* (2017) Paper-ID AIAA 2017-3245. doi:10.2514/6.2017-3245.

[8] Hasabnis, A., Maseland, H., Moens, F., Prachař, A. and Wild, J. Lessons Learnt from Chimera Method Application to a Deploying Krueger Device, *The 8th European Congress on Computational Methods in Applied Sciences and Engineering - ECCOMAS Congress 2022* (2022), Paper-ID 2246.

[9] Wallin, S., Montecchia, M., Eliasson, P. and Prachař, A. Scale-resolved simulations of the deployment and retraction of a Krueger high-lift device, *The 8th European Congress on Computational Methods in Applied Sciences and Engineering - ECCOMAS Congress 2022* (2022), Paper-ID 2245.

[10] Ponsin, J. and Lozano, C. Lattice Boltzmann simulation of a deploying Krueger device, *The 8th European Congress on Computational Methods in Applied Sciences and Engineering - ECCOMAS Congress 2022* (2022), Paper-ID 2213.